On nonstationarity and antipersistency in global temperature series

O. Kärner

Tartu Observatory, Tõravere, Estonia

Received 19 December 2001; revised 1 April 2002; accepted 10 April 2002; published XX Month 2002.

[1] Statistical analysis is carried out for satellite-based global daily tropospheric and stratospheric temperature anomaly and solar irradiance data sets. Behavior of the series appears to be nonstationary with stationary daily increments. Estimating long-range dependence between the increments reveals a remarkable difference between the two temperature series. Global average tropospheric temperature anomaly behaves similarly to the solar irradiance anomaly. Their daily increments show antipersistency for scales longer than 2 months. The property points at a cumulative negative feedback in the Earth climate system governing the tropospheric variability during the last 22 years. The result emphasizes a dominating role of the solar irradiance variability in variations of the tropospheric temperature and gives no support to the theory of anthropogenic climate change. The global average stratospheric temperature anomaly proceeds like a 1-dim random walk at least up to 11 years, allowing good presentation by means of the autoregressive integrated moving average (ARIMA) models for monthly series.

INDEX TERMS: 3309 Meteorology and Atmospheric Dynamics: Climatology (1620); 1610 Global Change: Atmosphere (0315, 0325); 1650 Global Change: Solar variability; 3250 Mathematical Geophysics: Fractals and multifractals; *KEYWORDS:* atmospheric temperature, solar irradiance, time series, nonstationarity, antipersistency

Citation: Kärner, O., On nonstationarity and antipersistency in global temperature series, *J. Geophys. Res.*, *107*(0), XXXX, doi:10.1029/2001JD002024, 2002.

1. Introduction

[2] Increase of knowledge about the variability of the Earth climate system is extremely important. Temperature is the main climate characteristic and an easily measurable physical quantity. It has been measured more than three centuries in some stations. The station data enable us to analyze the local climate variability. In order to estimate possible changes during last century, the global average temperature data sets have been collected using available surface air measurements. Collections by University of East Anglia Climate Research Unit (UEA CRU) [*Jones et al.*, 1999] and NASA GISS [*Hansen et al.*, 1999] are available online and widely used for climate research. Analysis of the ground-based temperature generally shows a remarkable global warming during recent decades [*IPCC*, 1996; *Jones et al.*, 1999]. But the ground-based data sets also contain a hardly removable uncertainty. Continuous temperature field over the Earth is very variable and the amount of stations was small hundred years ago in comparison of that today. UEA CRU online (www.cru.uea.ac.uk:80/cru/data) data set shows that only 18% of the Earth's surface was covered by stations in 1860 and the 40% level was not overtopped by the end of the nineteenth century. The situation compels to conclude that the obtained temperature values are of different accuracy. Several problems are connected to large-scale averaging of meteorological fields on the basis of discrete measurements. Temperature field has no smooth form but rather random and intermittent structure. There are lots of methods to estimate statistical structure in order to get optimal averaging schemes from discrete measurements [see *Kagan et al.*, 1997]. However, in the case where half of the area has no measurements at all during many years, they are rather useless. None of the methods can reproduce the actual average. The situation effectively reduces reliability of the ground-based global temperature series. It is reasonable to also analyze other and independent data sets.

[3] Temperature measurements using meteorological satellites opened a way to get methodically homogeneous and globally covered atmospheric temperature estimates. The data sets based on measurements by Microwave Sounding Unit (MSU) onboard polar-orbiting Tiros-N series satellites [*Spencer et al.*, 1990] of the stratospheric and tropospheric temperature are available since January 1979 on daily and monthly basis.

[4] Simultaneously, the solar irradiance measurements have been carried out using different radiometers and satellites. The results are collected, adjusted, cross-calibrated [*Fröhlich and Lean*, 1998a; *Fröhlich and Lean*, 1998b], and available online. Earlier attempts to find a direct statistical relationship between the solar activity and air temperature were unsuccessful [*Monin and Vulis*, 1971]. However, *Friis-Christensen and Lassen* [1991] recently found that the variation of the solar cycle length closely

0148-0227/02/2001JD002024$09.00

matches the long-term variation of the Northern Hemisphere land air temperature during the past 130 years. Modern precise series enable us to study the temporal variability of both the irradiance and temperature anomalies in more detail due to better temporal resolution.

[5] The aim of the present study is to analyze statistically the irradiance and temperature anomaly series in order to look into their variability and determine the properties important for climate research. Are the series stationary or nonstationary, persistent or antipersistent? What type of empirical models might be useful to represent them? Estimation of frequency distribution, correlation, spectral density, and R/S analysis are used to seek for the answers.

[6] In the appendix, modeling issues of the monthly mean temperature series are considered. The family of autoregressive integrated moving average (ARIMA) models is used to represent the monthly anomalies with a remarkably successful outcome in terms of residual variance. These models are shortly characterized by three numbers (p, d, q) where p denotes the order of autoregressive operator AR(p), q the order of moving average MA(q) part, and d shows the order of initial differencing [*Box and Jenkins*, 1976].

1.1. Stationarity Issues

[7] Quantitative characterization of random processes is inseparably connected to the terms stationarity and nonstationarity. According to mathematical definition [e.g., *Mandelbrot*, 1982], a process $x(t)$ is (strongly) stationary if the distribution of $x(t)$ is independent of t, the joint distribution of $x(t_1 + \tau)$ and $x(t_2 + \tau)$ is independent of τ, and similarly, for all k, the joint distributions of $x(t_1 + \tau), \ldots, x(t_k + \tau)$. The definition, involving all joint distributions, produces a too strong criterion and therefore, rules out most of the practical tasks for finite data sets. Thus, a more popular definition calls a process $x(t)$ (broadly) stationary if its mean value is constant and its autocovariance function is invariant under translation.

[8] Mathematical definitions are unique for all scales. Geophysical series are generally more complicate. The situation where both stationary and nonstationary behavior in a single data set occurs, but necessarily within different scaling ranges, small-scale nonstationarity and large-scale stationarity is inherent for several geophysical time series [*Davis et al.*, 1996a].

[9] In the present study, stationarity conditions for scale invariant time series are necessary, because satellite based temperature anomaly series are Brownian motion-like [e.g., *Kärner*, 1996], and the latter is a well-known scale invariant model. Spectral density $p(f)$ for a scale invariant process holds power-law behavior in considerable frequency scale $1/L_2 < f < 1/L_1$ [*Mandelbrot*, 1982; *Davis et al.*, 1996a; *Davis et al.*, 1996b],

$$p(f) \propto f^{-\beta}. \tag{1}$$

The value of β contains information about the degree of stationarity.

[10] Stationarity certainly holds for scaling processes with $\beta = 0$ (white noise). Using Wiener-Khinchine theorem about Fourier transform duality the spectral criterion for stationarity $\beta < 1$ can be established [*Davis et al.*, 1996a]. From that it follows that scaling processes with $1 < \beta < 3$ are nonstationary with stationary increments. In the present study these conditions are used to classify the global daily temperature and solar irradiance series. Whereas a 22-year record is quite short in comparison with an ordinary understanding about climate scale, the results have less climatic importance per se and more methodical character in order to better understanding about the variability structure in the Earth climate system.

1.2. Persistency or Antipersistency in a Data Set

[11] Important climatological information can be obtained separating scale invariant temperature series according to the growing rate of the rescaled range of their trajectories. *Hurst* [1951] initiated the rescaled range studies for natural time series and started to characterize its growing rate by the exponent H, $0 < H < 1$.

[12] His work stimulated *Mandelbrot and Van Ness* [1968] to introduce more general process than Brownian motion. They defined a process called fractional Brownian motion (fBm), $B_H(t)$, $-\infty < t < \infty$ with parameter H ($0 < H < 1$) such that $B_H(t_2) - B_H(t_1)$ has zero mean and variance $|t_2 - t_1|^{2H}$. In the case of $H = 0.5$ the process coincides with the ordinary Brownian motion.

[13] FBm has an important property, significant long-range correlation between its nonoverlapping increments. The correlation turns out to be positive if $H > 0.5$ and negative if $H < 0.5$ for all lags up to infinity. If $H > 0.5$ the increments tend to have the same sign, so that $B_H(t)$ tends to increase in the future if it has had an increasing tendency in the past. The feature is called persistency. Physically, a persistent system is going to increase a deviation showing a positive feedback dominating in the system governing the series. If $H < 0.5$, the increments $B_H(t_2) - B_H(t_1)$ and $B_H(t_3) - B_H(t_2)$ during the nonoverlapping time intervals $t_1 < t_2 < t_3$ ($t_2 - t_1 = t_3 - t_2$) tend to be of opposite sign, so that $B_H(t)$ has a tendency to decrease in future if it has had an increasing tendency in the past and vice versa. The feature is called antipersistency. The antipersistency expresses a tendency of the values of increments to compensate for each over to prevent for the trajectory from blowing up too fast. Such a system tends to eliminate deviations showing a negative feedback in aggregate. An antipersistent time series visit, on average, the mean value more often than an ordinary Bm. *Mandelbrot and Wallis* [1969] showed that the perfect compensation occurs in pure sine wave leading to $H \to 0$ if $\tau \to \infty$. Actually, the limit (if $\tau \to \infty$) may or may not exist, but nevertheless, the sample based value of H exists, indicating independence of increments or departure towards persistency or antipersistency during the sampling time.

[14] Thus, the value of H (less or more than 0.5) determines the long-range behavior of the time series. Estimation of H becomes the first task. This important parameter has many names in the scientific literature: the Hurst exponent, the self-similarity, or the intensity of long-range dependence parameter. In section 4 the actual estimation of H for the temperature and irradiance series is carried out and results presented.

[15] Note that the terms persistency and antipersistency are originally determined for (stationary) increments of a (nonstationary) series (see *Mandelbrot* [1982], p. 251 for details). There holds the direct analogy with the ordinary

Brownian motion which is defined via its (independent and identically distributed) increments. If the increments are nonstationary, the obtained H value has no meaning in relation to its defined sense. Overlooking this condition may lead to misinterpretation of the terms, as one can see in work by *Koscielny-Bunde et al.* [1998].

2. Data

[16] Global temperatures have been monitored by satellite since 1979 [*Spencer et al.*, 1990] with the Microwave Sounding Units (MSU) flying on the National Oceanic and Atmospheric Administration's (NOAA) TIROS-N series of polar-orbiting weather satellites. Data of the thermal emissions of radiation by molecular oxygen at four frequencies near 60 GHz from nine separate satellites have been combined to provide a global record of temperature fluctuations in the lower troposphere (the lowest 8 km of the atmosphere) and the lower stratosphere (covering an altitude range of about 15–19 km). [*Spencer and Christy*, 1992a; *Spencer and Christy*, 1992b] have shown that the MSU calibrations have been very stable, with a precision of monthly satellite measurements of 0.02°C for the global mean.

[17] Revisions to previous version of these data sets have been recently applied to account for the effects of orbit decay (loss of satellite altitude) and orbit drift (east-west movement) [*Christy et al.*, 2000]. Orbit decay introduces an artificial cooling in lower tropospheric temperature data set, while the effects of orbit drift introduce artificial warming. The change in global trends due to these operations for 1979–1998 for lower tropospheric temperature was an increase from +0.03 to +0.06 K per decade.

[18] A comprehensive comparison is made by *Hurrell et al.* [2000] between two tropospheric temperature data sets over the period 1979–1998: the most recent and substantially revised MSU channel 2 data retrievals, and a gridded radiosonde analysis provided by the Hadley Center of the U.K. Meteorological Office. The latter is vertically weighted to approximate the deep layer temperatures measured by the satellite data. At individual grid points, there is good overall agreement among monthly anomalies, especially over the Northern Hemisphere continents where the climate signal is large, although monthly root-mean-square (rms) differences typically exceed 0.6°C. Over the tropics, correlations are lower and rms differences can be as large as the standard deviations of monthly anomalies. Differences in the grid point variances are significant at many locations, which presumably reflects sources of noise in one or both measurement systems. For collocated global average monthly anomalies, correlations are 0.9 with rms differences 0.10°C for both lower tropospheric and midtropospheric anomalies [*Hurrell et al.*, 2000].

[19] The global daily and monthly averaged temperature anomalies for the entire period of record (since January 1979) are available online (www.ghcc.msfc.nasa.gov/). Two daily records, T_{tr}, the average temperature anomaly for lower troposphere (6–8 km deep), and T_st, the average stratospheric temperature anomaly series for the time interval from January 1979 to August 2001, are analyzed in the present study. Missing data (total amount is 76 days during the period from 1979 to 1991, with the longest interval of 15 days) are interpolated linearly. The operation decreases variance for the studied series, but enfolding less than 1% of the whole data set, the resulting bias is negligible.

Table 1. Estimated First Moments for the Series T and I and Their Increments dT and dI

Data Type	Unit	n, days	Sample Mean	Standard Deviation
T_{st}	°C	8279	0.01339	0.50441
dT_{st}	°C	8278	−0.00012	0.01858
T_{tr}	°C	8309	−0.00703	0.21631
dT_{tr}	°C	8308	0.00000	0.03752
I	Wm^{-2}	7988	1366.223	0.59741
dI	Wm^{-2}	7987	0.00026	0.18215

[20] A composite record of the sun's total irradiance (I in Wm^{-2}) compiled from measurements made by five independent space-based radiometers since 1978 and adjusted for drifts in the radiometric data by *Fröhlich and Lean* [1998a] is available online. The composite record exhibits a prominent 11-year cycle with similar levels during 1986 and 1996, the two most recent minimum epochs of solar activity. *Fröhlich and Lean* [1998b] emphasize that no irradiance increase from 1986 to 1996 solar minima. Nor does the irradiance record support a recent upward irradiance trend inferred from solar cycle length. The data set contains daily irradiance values from 1978 to 2000. Missing daily values are interpolated for spectral density calculations and R/S analysis.

3. Statistical Characteristics for Daily Series

3.1. First Moments

[21] Standard formulae to calculate sample mean, variance, correlation function [e.g., *Box and Jenkins*, 1976] are used in the present section. Estimates of sample mean and variance for the temperature and irradiance daily anomaly series (T_x and I, respectively) and their daily increments (dT_x and dI), together with values of sample size n, are shown in Table 1. Sample mean values for the temperature anomalies are nonzero because the anomalies are originally calculated in respect to the 20-year interval, but we are using the maximum available record (more than 22 years). The stratosphere tends to cool and the solar irradiance to increase during that period. Note also a remarkably small variance for the daily increment series in comparison with that for the anomaly series.

[22] Autocorrelations $r(k)$ for lags $k = 0, 1, \ldots, 100$ days, calculated for two temperature anomaly series X_i and their daily increments $x_i = X_i - X_{i-1}$, $i = 1, \ldots, n$ are shown in Figure 1.

[23] Autocorrelations for the daily stratospheric temperature anomalies decay extremely slowly. Autocorrelations for two other series show a bit faster decay during the first lags up to 10 days. Then a similarly slow decay goes on. Daily increments are much less correlated. Only a few first values appear to be remarkably nonzero. Behavior of the autocorrelations for I and dI are very similar to those for T_{tr} and dT_{tr}, respectively (not shown).

3.2. Distribution of Daily Anomaly and Increment

[24] Frequency distributions for three studied series are shown in Figures 2a–2c.

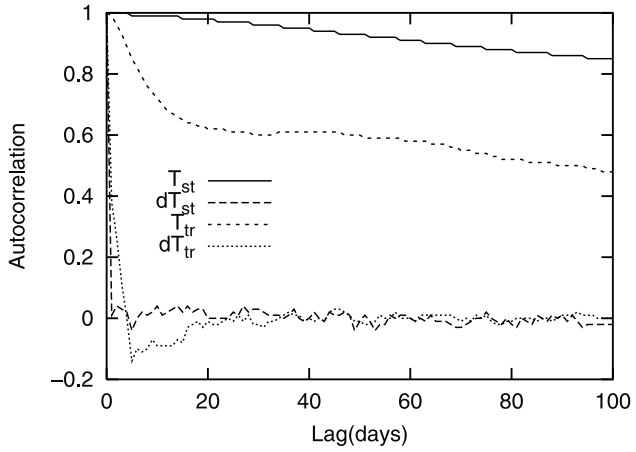

Figure 1. Sample autocorrelations for the global temperature anomalies (T_x) and their daily increments (dT_x).

[25] As a rule, the daily anomalies have asymmetric and often multimodal probability distribution density with large variance. On the other hand, estimated sample densities for the increments are unimodal, nearly symmetric, and have about a magnitude less variance in comparison with the anomalies. Some asymmetry is observed in distribution of the irradiance increments. Testing estimates for asymmetry and excess shows that the increment distributions are different from the normal distribution at 95% significance (not shown) in two cases. The same result was obtained using Kolmogorov-Smirnov (K-S) test between hypothetical normal distributions with the estimated sample mean and variance (see Table 1) and the empirical frequency distribution. Actual maximum differences for dT_{tr} and dI are 0.020 and 0.099, respectively, but the 95% critical value equals to 0.015. The distributions are characterized by a high peak at the mean and fatter tails than normal distribution having the same variance. The current dT_{st} sample appears to be approximately normal (i.e N(0, 0.019)) at the 95% level.

3.3. Running Standard Deviations

[26] Temporal variability of variance is an important topic for determining the time series modeling opportunities. Running standard deviation estimates are calculated for six variables (for anomalies and their increments) and the most interesting features are shown in Figures 3a and 3b. Figure 3a shows dependence of the standard deviations for temperature and irradiance anomalies as functions of record length. The log/log scale figure indicates that standard deviations for the anomalies are increasing together with the increasing record length τ with different speed.

[27] Figure 3b shows standard deviation time series estimated for 268 nonoverlaping 30-day-long intervals. Only four lines are shown. Variability of the estimates for dT_{tr} and dT_{st} is very weak and thus not shown. The results do not contradict possibility that both temperature anomaly series have stationary increments. 30-day standard deviation records for T_{tr} and T_{st} vary slowly with approximately similar amplitude and opposite phase.

[28] Variability in the irradiance record is more complicated. Both irradiance anomaly and its daily increment represent series with time varying variances. The variance is increasing during the period of increased solar activity and vice versa. Standard deviation records for anomaly and its increment change nicely in the same phase. The both standard deviations have quite similar values during the periods of low solar activity and differ remarkably otherwise. Figure 3b also reveals that the transition period from high to low variance may be abrupt (July 1984) or slow (1994). This is the first statistic found where the T_{tr} and I series behave essentially differently.

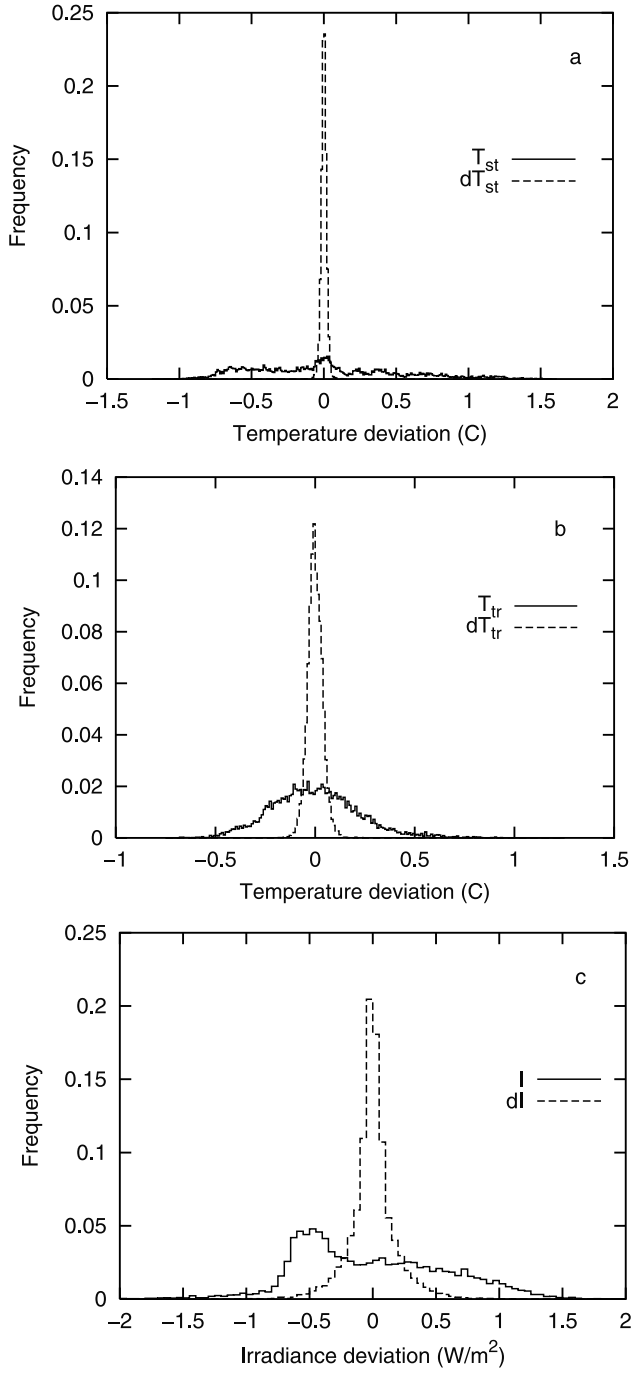

Figure 2. Frequency distributions for the anomaly and increment samples for (a) stratospheric temperature, (b) tropospheric temperature, and (c) irradiance.

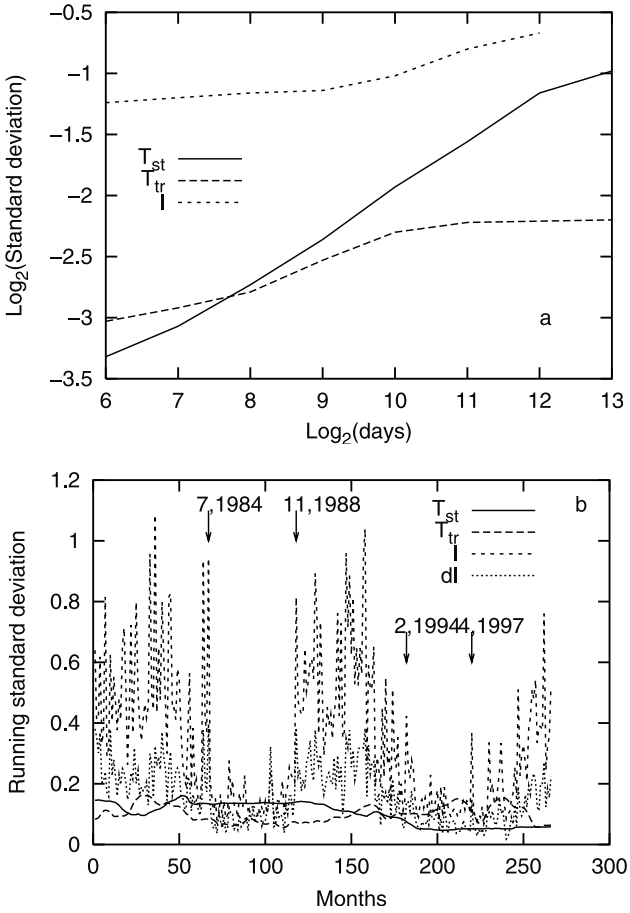

Figure 3. Running standard deviations calculated (a) for increasing time interval in log/log scale, and (b) for non-overlapping constant $\tau = 30$ day sequences of the anomaly and increment series. Month and year of the abrupt changes in the irradiance record are marked with arrows.

3.4. Spectral Density

[29] Spectral density $p(f)$ is calculated using of the routine SPCTRM by *Press et al.* [1993]. Bartlett window function is used in it. Choice of the window type is not important in our case. To reduce statistical noise, the average of two estimates each calculated for 4096 points is presented. The cost of this approach is loss of information at the large scales. Smoothed spectral density estimates in logarithmic scale $log_2 p(f)$ are shown in Figure 4a for the daily anomalies and in Figure 4b for the increments. Log_2 is used because it facilitates counting periods starting from the Nyquist frequency ($log_2 f = -1$) to whole interval ($log_2 f = -12$). They correspond to the periods 2, 4, . . ., 4096 days.

[30] Low frequencies are dominating in the variability of all three daily anomaly series. An approximate power-law behavior holds for the main interval of frequencies ($-10 \leq log_2 f \leq -1$) available from the current anomaly records. Estimated values for the scaling exponent β in equation (1) equal to 2 (T_{st}), 1.75 (T_{tr}) and 1.5 (I). All anomaly series appear to be nonstationary with stationary daily increments in the corresponding timescale.

[31] Determined high-frequency limit for nonstationarity is presumably technical due to the daily sampling. Synoptic scale motions in the troposphere are covering the scale from some hours to a week and the β value for turbulent energy dissipation spectral density is 5/3. A close exponent value ($\beta = 1.8$) has been found for several ground based temperature records in *Lovejoy and Schertzer* [1986] extending to at least several minutes to month. The present estimate for the mean tropospheric temperature anomaly appears also to be close to those.

[32] Obtained $\beta = 2$ estimate for T_{st} over a considerably wide frequency interval corresponds to that for Brownian motion (Bm), but the spectral density does not determine a process uniquely [*Davis et al.*, 1996a].

[33] Spectral density estimates for dT_{st} show that the similarity with Bm continues. The graph is close to that for white noise, ($p(f) \approx const$) over the whole available interval. Two other increment series have more complicated spectra. Higher frequencies associated with 8–32 day periods are evidently dominating in both cases. The situation seems to be natural, because energetically strong annual course in the solar irradiance (in comparison with the daily anomalies) suppresses lower frequency Fourier modes for the increment series. Note that difference between the T_{tr} and T_{st} spectral behavior is larger than that

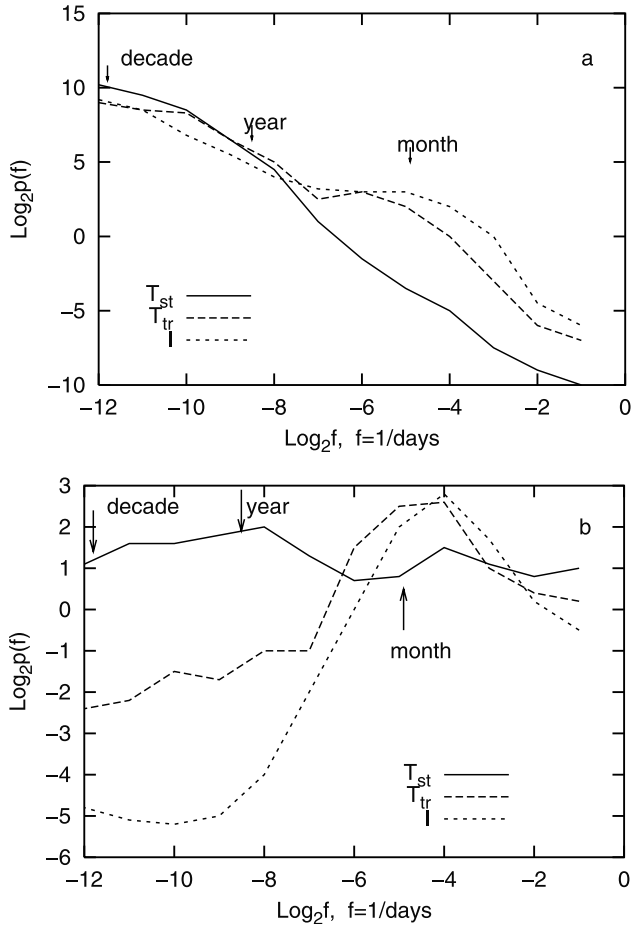

Figure 4. Smoothed spectral density estimates (a) for three daily anomaly series and (b) for their daily increment series in log/log scale. Here f = 1/days; that is, -1 corresponds to Nyquist frequency (2-day period), and -12 to 4096-day period.

between T_{tr} and I. The same situation holds for most of the calculated statistics.

4. Detection of Long Memory

[34] Results show that the temperature anomaly series behave like nonstationary processes with stationary increments. Estimating H is the next important step to characterize the samples of the series. The result enables us to separate nonstationary scale invariant processes with stationary increments (i.e, $1 < \beta < 3$) into different groups depending on H. Such a separation is useful for monitoring the temperature (irradiance) anomaly development and helps to distinguish between situations where positive or negative correlation (or lack of it) dominates in the physical system generating the series.

[35] Methods to estimate long-range dependence by means of H are rapidly developing during the last decade. Technically, one can use both the anomalies and increments for that. Due to large variance of spectral estimates the results from previous section are not used for that purpose. Instead of that, two other independent schemes are used for estimating H on the basis of 22-year daily time series: R/S analysis and regression on the periodogram. The former is one of the oldest methods (its graphical presentation gives a picture about possible dependence of H on block size), and the latter is certified by *Taqqu and Teverovsky* [1996] to be one of the most robust methods for this task.

4.1. R/S Method

[36] The R/S method is one of the better known methods for estimating H. It is discussed in detail by *Mandelbrot and Wallis* [1969].

[37] The letters R/S stand for the rescaled range $R_{i,\tau}/S_{i,\tau}$, where $R_{i,\tau}$ is the cumulated range of a process between times $i + 1$ and $i + \tau$ after removal of the sample average and $S^2_{i,\tau}$ is the corresponding sample variance. That is, for a series x_i in discrete integer valued time with X_i defined by $X_i = \Sigma^i_{j=1} x_j$, and given any lag $\tau > 1$, $R_{i,\tau}$ is defined by

$$R_{i,\tau} = \max\left[\left(X_{i+j} - X_i\right) - (j/\tau)(X_{i+\tau} - X_i)\right] - \min\left[\left(X_{i+j} - X_i\right) - (j/\tau)(X_{i+\tau} - X_i)\right], \quad (2)$$

where max and min are taken over $0 < j < \tau$. Let $S^2_{i,\tau}$ be the corresponding sample variance,

$$S^2_{i,\tau} = \tau^{-1} \sum_{j=1}^{\tau} x^2_{i+j} - \left(\tau^{-1} \sum_{j=1}^{\tau} x_{i+j}\right)^2,$$

then the rescaled range $\Re_\tau$ is defined as follows:

$$\Re_\tau = E\left[R_{i,\tau}/S_{i,\tau}\right], \quad (3)$$

where the averaging is over nonoverlaping intervals of length τ going in the available interval $i = 1, \ldots n$.

[38] Actual calculation of the rescaled range is convenient to produce over nonoverlapping time intervals τ, 2τ, 4τ, etc. Averaging in equation (3) is then over the number of intervals of each length fitting in the all available interval. The longest interval gives a single $\Re$ estimate. On the basis of averaged $\Re_\tau$ values, estimate of the Hurst exponent H can be easily computed fitting a linear equation

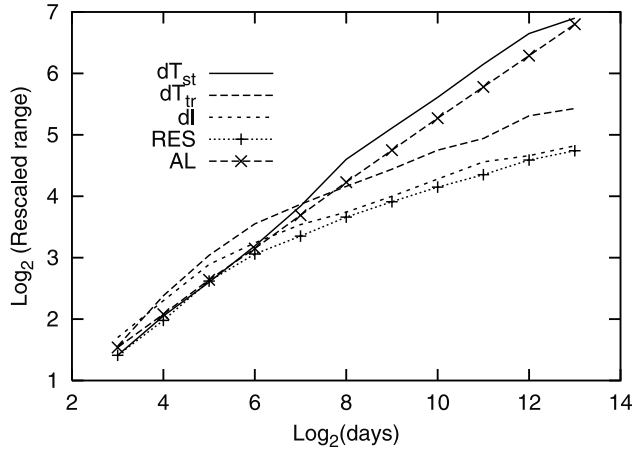

Figure 5. Rescaled range $\Re_\tau$ results (τ in days) for three increment series and MA(3) residuals (label RES) together with values computed by Anis-Lloyd equation (5) (AL).

$$\log_2(\Re_\tau) = A + H \log_2(\tau) \quad (4)$$

by least squares over the interesting τ interval. Obtained solution $\hat{H}$ for equation (4) shows the average slope over the used τ interval. Value of the intercept A is less important in our case. Log_2 is used again in order to have the same scale division with the spectral densities.

[39] The R/S calculations are carried out for three series using dI, dT_{st} and dT_{tr} as x_i values for equation (2), respectively. The following block size τ values (in days) are used: τ = 16, 32, 64, 128, ..., 8192. The averaged $\Re_\tau$ values are plotted in Figure 5 in log/log scale.

[40] Unfortunately, the $\tau^{0.5}$ law does not hold precisely for short series if $\Re_\tau$ is calculated from pseudo random numbers. It is due to systematically lower $\Re_\tau$ values obtainable by means of differently generated pseudorandom variables for shorter series (i.e., those with length in a few hundred points). *Anis and Lloyd* [1976] developed the following approximate equation to circumvent the systematic deviation of the $\Re_\tau$ value for small τ:

$$E(\Re_\tau) = \sqrt{\frac{2}{\tau\pi}} \sum_{j=1}^{\tau-1} \sqrt{(\tau - j)/j}. \quad (5)$$

[41] $\Re_\tau$ values for the lags used in the present study calculated by means of equation (5) are shown in Figure 5 (with label AL).

[42] For finite series $\Re_\tau$ is sensitive to short-range correlation in initial series. A simple method to eliminate this is to fit some ARIMA type model to initial series and afterwards use R/S analysis to the residuals. The process is carried out with dT_{tr} data set using MA(3) model. The approach is justified, because three first sample autocorrelations for dT_{tr} (see Figure 1) are remarkably nonzero The approach is sufficient to remove the short-run correlation (not shown). $\Re_\tau$ estimates are calculated for the residuals over the same grid for τ as previously. The results are marked in Figure 5 with label RES. They show that the

Table 2. Estimated H Values for Three Series by Two Methods

Parameter	T_{st}	T_{tr}	I
n, days	8192	8192	7882
$\hat{H}_{R/S}$	0.57	0.27	0.23
$\delta H_{R/S}$	±0.04	±0.04	±0.04
M, frequencies	400–800	400–800	200–400
Min H_{Per}	0.54	0.26	0.25
Max H_{Per}	0.58	0.36	0.35
δH_{Per}	±0.06	±0.06	±0.09

model shifted $\Re_\tau$ values for all intervals. However, calculating partial H values between successive points confirms that these H estimates remain unchanged in respect to those for dT_{tr} for longer lags if $log_2\tau > 8$. The straight line sections of $\Re_\tau$ for dT_{tr} and RES are nearly parallel if $\tau > 256$. The MA(3) model is incapable to change the behavior of $\Re_\tau$ for longer time lags (i.e., to represent a long-run dependence). The growing rate in both cases is evidently slower than that for Bm indicating $H < 0.5$. In terms of empirical modeling the result does not support using ARIMA family for modeling the daily anomaly series temporal variability.

[43] Average values over the straight part (i.e $\tau \geq 64$) of the $\Re_\tau$ curves together with the corresponding δH by R/S analysis are shown in the third and fourth row of Table 2, respectively. Here δH denotes the approximate 95% confidence interval ($\pm 1.96\sigma$) around the estimate. Here $\sigma = 0.02$ is the empirical estimate obtained independently by *Bassingtwaite and Raymond* [1994] and *Taqqu et al.* [1995] on the basis of various model calculations for the case $H = 0.5$ and maximum of $\tau \approx 10000$.

4.2. Regression on the Periodogram

[44] This method is useful, because of known asymptotic variance of the obtainable $\hat{H}$ (see *Taqqu and Teverovsky* [1996] for discussion). The method is based on the periodogram (i.e., an estimator of the spectral density) of the time series, defined by

$$p(f) = \frac{1}{n}\left|\sum_{j=1}^{n} x_j e^{2\pi ijf}\right|^2, \qquad (6)$$

where f is frequency, n is the number of terms in the series, and x_j are the data. A series with long-range dependence has a spectral density proportional to $|f|^{-\beta}$, close to the origin, where $\beta = 2H - 1$. Thus, a regression of the logarithm of the periodogram versus the logarithm of the frequency should give a coefficient of $1 - 2H$. Note that here we use increments instead of anomalies. Because of this, the corresponding β value is smaller by two in comparison with that in the first formula. Since the proportionality to $|f|^{1-2H}$ holds only for f close to the origin, finding the right cut-off is very important. Let M be the number of frequencies used for the regression. Using large values of M, we may find a range where the estimates of H are incorrect because of the short-range effects. Moving to small M value we will get into a region where the estimates of H are very scattered and unreliable because there are not enough frequencies left to have an accurate regression.

[45] Still no method has been found to determine the right cutoff M value a priori. Following [*Taqqu et al.*, 1995], the lowest 10–20% of the roughly $n/2 = 4096$ (temperature) and $n/2 = 2048$ (irradiance) frequencies are used since the proportionality above holds for f close to the origin. On the basis of that frequency interval, maximum and minimum of the H estimates are determined and are shown in Table 2 together with the corresponding δH values. The δH denotes the approximate 95% confidence interval ($\pm 1.96\sigma$) around the estimate. Here $\sigma = \pi/\sqrt{24M}$ is the asymptotic standard deviation calculated by *Robinson* [1995].

4.3. Results for the Daily Increment Series

[46] Figure 5 shows the dependence of $\Re_\tau$ on τ according to equation (4). For short lags ($\tau \leq 32$ days), all three $\Re_\tau$ curves are approximately parallel to that with the label AL. For longer lags, the curves depart significantly. Behavior of the global average stratospheric temperature anomaly is still looking close to a Bm sample path, as long as the scale is up to 4096 days. The estimated H values remain close to 0.5 for that scale. Table 2 values together with their estimated confidence intervals fully support that result.

[47] In the stratosphere, dynamics, radiation, and photochemistry are coupled in a complicated feedback loop which retains its radiative equilibrium [e.g., *Staehelin et al.*, 2001]. The loop also generates weakly correlated daily temperature increments for the globally averaged stratospheric layer between 15 and 19 km (i.e., the layer covered by MSU observations). The antipersistence in the daily irradiance values has no visible effect to the stratospheric temperature fluctuations. Probably the Chapman cycle of ozone production does not depend significantly on daily variations in irradiance because all solar energy in wavelengths shorter than 242 nanometers is absorbed by ozone anyway. The corresponding daily variations are small in comparison with the whole energy in that spectral band.

[48] In Figure 5, a noticeable turn towards antipersistence of the stratospheric $\Re_\tau$ curve can be seen for the largest τ interval (i.e., between 4096 and 8192 days). Might this be an indication about the existence of integral scale between small-scale nonstationarity and large-scale stationarity? Physical mechanism behind the possible scale break may be connected to stratospheric ozone [*Robock*, 1996]: Most of the total solar irradiance variations over an 11-year sunspot cycle is in ultraviolet wavelengths, which are absorbed by the ozone in the stratosphere. The ozone production is also dependent on solar cycle. The amplitude of the global mean total ozone variation from solar minimum to solar maximum is 1.5% to 2% and 85% of that change occurs in the lower stratosphere [*Hood*, 1997]. The process introduces a cyclic forcing to the stratosphere and thus slows down the growing rate for $\Re_\tau$ in comparison with that for random walk. Because there is only one observation for the scales longer than 11-year solar cycle, the question about the scale break in the stratospheric temperature anomaly series remains open. The appeared antipersistency might be an influence of the cyclic solar forcing to the rescaled range, or just a deviation due to considerable variance of the $\Re_\tau$ estimates. For a more precise answer, we need to await the data set growing during at least one more solar cycle.

[49] Figure 5 shows that the lower tropospheric temperature and irradiance increments are evidently antipersistent for τ values 64 (days) and longer. H estimates for dT_{tr} and dI are close to each other for all available scales. Figure 5

and Table 2 do not contradict the possibility, that the Hurst exponent might have constant value $H = 0.25$ during a considerably long temporal interval from 2 months to 20 years. Tropospheric temperature is closely related to the surface air temperature. Long-term fluctuations (i.e., annual cycle removed) of the latter are studied by *Lovejoy and Schertzer* [1986]. They used two different data sets of monthly averaged temperatures over the Northern Hemisphere. Their result, $H = 0.4$ for $\tau \geq 5$ years, is somewhat larger. At least a part of the difference is due to technical reasons. Monthly averaged ground based data sets are more noisy than the satellite records. It is reasonable to assume that the averaging grid (spatial and temporal) is independent of temperature. If the H estimate for a pure signal is less than 0.5, then an additional white noise component increases it. As a result the estimates are in reasonable accord and both methods are obviously pointing to the antipersistency.

[50] Variability of the daily irradiance and tropospheric temperature anomaly increments is similar in terms of H on the basis of spectral density, R/S analysis, and periodogram regression. Relationship between (main) forcing and response becomes evident on that level. Variability of the solar forcing is quite accurately followed by tropospheric temperature anomaly. This is an indication that the solar forcing variability is actually the governing one among other existing (random or not) forcings in the Earth climate system. Variations in the Earth climate system also give rise to changes in the radiation budget at the top of the atmosphere. Such variations may be separated into two groups: those having trends during several decades and those being periodic or random. The first group describes long-term tendencies in the atmosphere (e.g., growing of the concentration of CO_2 and other greenhouse gases or on the land such as the decrease of the lake Chad area from 25,000 to 1350 km^2 during 35 years [*Coe and Foley*, 2001]). The second group is mainly connected to the interannual changes in geographical distribution of snow, ice, and cloudiness. Strong fluctuations of the radiation budget both at the top of the atmosphere and at the surface are caused by cloudiness. Cloud fields are highly transitory in spatial scales about 1000 km or smaller [*Cahalan et al.*, 1982], but show certain systematic behavior if zonal variability is considered [*Kärner and Rannik*, 1996]. However, the information is still insufficient for estimating the average radiation budget variability due to cloudiness changes.

[51] Very similar values for H for I and T_{tr} over the analyzed time interval indicate that the atmospheric and ground-based forcing fluctuations should be quite random in aggregate. They have no power to change the antipersistent behavior declared by the irradiance variability.

[52] Simple comparison for the obtained H values can be produced counting zero crossings. The days i and $i + 1$ where X_i and X_{i+1} have different signs determine at least one zero crossing for the continuously varying temperature anomaly sample path. The amount of such crossings should be higher for T_{tr} (as a sample of an antipersistent process) than for T_{st} (that close to Bm). Counting sign changes for daily values during 8278 days gives 131 for T_{st} and 442 for T_{tr}. This is an independent result to confirm that the current T_{tr} trajectory is produced by means of increments with stronger anti-persistence than that for T_{st}. Similarly, crossings the mean value of the irradiance are counted,and the result, 525 is close to that for the tropospheric temperature.

5. Summary and Climatic Relations

[53] Behavior of the studied temperature and irradiance time series appears to be nonstationary. Daily increments for the temperature anomaly series are stationary, weakly correlated, and close to normal for the lower stratosphere. Daily increments for the solar irradiance anomaly are nonnormal with varying variance depending on solar activity. An essential difference is revealed in the long-range behavior of the series. Estimates of the Hurst exponent enable one to make a few conclusions about the contemporary global average climate and human influence to it.

[54] Determination of stationary or nonstationary behavior in temporal variability of climate variables over a sufficiently broad scale is important for climate definition. Although one dimension (temperature) is not sufficient for satisfactory description of climate it is useful to explain the problems connected to the definition. Climate is often determined using statistical tools, for example, "the climate is represented by the statistical collective of its weather conditions during a specified interval of time" [*Huschke*, 1959], or "is ensemble of states visited by the Earth climate system during a few decades" [*Monin*, 1982].

[55] The available satellite records are too short, but as time goes on there might be a specific scale, at which the Fourier modes stop increasing with scale and become constant. It is known as an integral or correlation scale L_I [*Davis et al.*, 1996a]. The integral scale L_I separates scales where $\beta < 1$ from those where $\beta > 1$ thus defines the threshold between large-scale stationary and small-scale nonstationary regimes. If $L_I < \infty$ exists, a specified interval of time can be connected to it with a rational hope that the sample mean values for climate variables converge if averaged over larger than L_I scale provided that the climate does not change. In this case we have a quantitative basis to characterize the climate for a certain epoch.

[56] These hopes cannot still be very promising, at least for the tropospheric temperature. Previous analysis of the Northern Hemispheric temperature records by *Lovejoy and Schertzer* [1986] and recent study of climatic records from the Greenland ice-core project [*Schmitt et al.*, 1995] do not find any sign of L_I. *Ghil* [2001] points out that climate varies in all timescales. If these variations bring about nonstationarity, there is a danger for the term climate to retain only some qualitative sense which does not help to determine the possible human-induced climate change. In order to get a practically meaningful definition of climate it may be reasonable to change the words "ensemble of states" to "ensemble of increments with a certain Hurst exponent." Instead of trying to characterize the climate via nonstationary, anomalies simply change to use of stationary increments (existing for the global temperature, at least). Determining the Hurst exponent helps to quantify their long-range dependence. Stationary processes have so many useful properties in comparison with nonstationary ones that the idea might be worth of research. The frequency distributions in Figures 2a and 2b show that increment distributions have much simpler form and can be more easily approximated by means of theoretical curves.

[57] The revealed antipersistence in the lower tropospheric temperature increments does not support the science of global warming developed by *IPCC* [1996]. Negative long-range correlation of the increments during last 22 years means that negative feedback has been dominating in the Earth climate system during that period. The result is opposite to suggestion of *Mitchell* [1989] about domination of a positive cumulative feedback after a forced temperature change. Dominating negative feedback also shows that the period for CO_2 induced climate change has not started during the last 22 years. Increasing concentration of greenhouse gases in the Earth atmosphere appeared to produce too weak forcing in order to dominate in the Earth climate system. Estimate of the adjusted radiative forcing due to changes in the concentrations of the so-called greenhouse gases since preindustrial times is 2.45 Wm^{-2} [*IPCC*, 1996]. If the increase was during 15 years, its annual increment (0.16 Wm^{-2}) would be comparable to standard deviation of the daily increment of solar forcing at the top of the atmosphere (0.18 Wm^{-2}). The observed global warming in surface air temperature series [*Jones et al.*, 1999] is more likely produced due to overall nonstationary variability of the Earth climate system under anti-persistent solar forcing.

Appendix A: ARIMA Representation for Monthly Temperature Anomalies

[58] The dT_{st} series appear to be approximately normally distributed and weakly correlated at least during one solar cycle. This means that Bm (more precisely, ARIMA (0, 1, 0) or random walk for current discrete series) should be an acceptable model to represent the global mean stratospheric temperature anomaly temporal variability, at least for series shorter than one solar cycle. In this section an ARIMA model is fitted to both monthly temperature series dT_{st} and dT_{tr}. The global monthly data sets are used to ease the calculations. The averaging adds one necessary MA term to initial model (because of the averaging grid is independent of the temperature), and (0, 1, 1) model is fitted. The same model has been earlier used by *Kärner* [1996] to represent temporal variability for several monthly series. The goal here is not to seek for the best approximation but to demonstrate an applicability of the simplest model.

[59] For monthly increments $x_i = X_i - X_{i-1}$ the model takes even simpler form (0, 0, 1),

$$x_i = m_0 + a_i - \Theta_1 a_{i-1}, \tag{7}$$

where a_i ($i = 1, 2, \ldots, n_1$) is white noise and Θ_1 is fitted by least squares. Constant m_0 stands for the existing trend (mean monthly increment in our case) in the initial sample. The estimated trends are available online and m_0 estimates for $n_1 = 265$ month series are equal to 0.0002°C (T_{tr}) and −0.005°C (T_{st}). This means that there has been slight warming in lower troposphere and a bit stronger cooling in stratosphere during the last 22 years. It is too small trend to cause an essential error for short-range approximation and it is neglected in further calculations. Parameters for the fitted models are shown in Table A1, where S_X^2 and S_a^2 stand for initial (i.e., that for the monthly anomaly data) and residual variance, respectively.

Table A1. Model (7) Fitting Results for Monthly Mean Series

Data	Time	n_1, months	Θ_1	S_a^2	S_a^2/S_X^2	Q
dT_{st}	1979–2001	264	−0.501	0.0103	0.04	28.3
dT_{tr}	1979–2001	264	0.354	0.0129	0.35	22.4

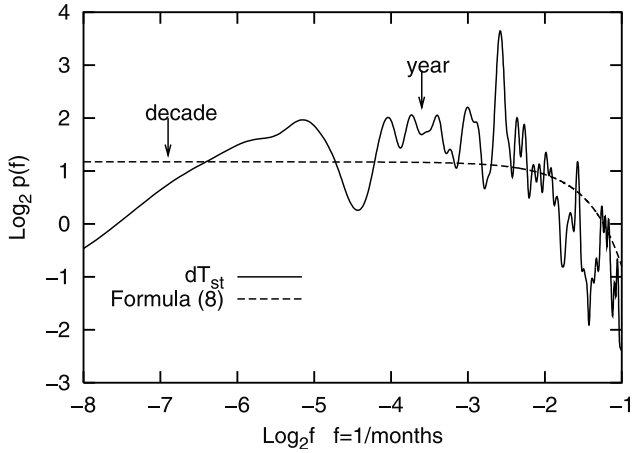

Figure A1. Empirical and model (8) determined spectral densities for monthly stratospheric temperature increment series.

[60] Θ_1 values fitted to dT_{tr} and dT_{st} series have different signs. This feature introduces a big difference in the time series behavior. Power spectrum for a MA(1) model can be written as [*Box and Jenkins*, 1976]

$$p(f) = 2\left(1 + \Theta_1^2 - 2\Theta_1 \cos 2\pi f\right), \quad 0 \le f \le 0.5. \tag{8}$$

Equation (8) shows that if $\Theta_1 < 0$ (dT_{st}) lower frequencies are dominating and if $\Theta_1 > 0$ higher frequencies are dominating in the spectra.

[61] Estimated and model determined (with $\Theta_1 = -0.501$ from Table A1) spectral densities for the stratospheric series are shown in Figure A1 in log/log scale. Comparison of Figures 4b and 6 shows the scaling properties for the stratospheric temperature anomaly are changed for the monthly averaged series in comparison with those for daily ones. The same is valid for dT_{tr} (not shown). Results by [*Pelletier*, 1998] calculated from different station data show that similar changes are likely if going from the global average towards smaller spatial scale.

[62] Frequency distributions for the monthly increments and residuals appear to be close to normal (not shown). The result may be valid for short series (n1 = 264 months) only. There are actually two comparatively large jumps in the stratospheric temperature anomaly data set, corresponding to El Chichon (April 1982) and Pinatubo (August 1991) eruptions [*McCormick et al.*, 1995], respectively. However, in the case of 265 observations, two large deviations can not prevent passing the K-S test. Nevertheless, the physical basis for long-run nonnormality due to large volcanic eruptions obviously remains. Another considerable feature is that no large jump occurred in the daily temperature increments during the eruption days or even during the following week. Only after some accumulation time the

average stratospheric temperature responded. The response is clearly distinguishable in monthly series (www.ghcc.msfc.nasa.gov/temperature).

A.1. Diagnostic Testing

[63] Any test is needed to get an idea about adequacy of the fitted models. It has been shown [e.g., *Box and Jenkins*, 1976] that for a satisfactory model, the variable

$$Q = N \sum_{k=1}^{K} r_a^2(k), \tag{9}$$

where $r_a(k)$ are estimated autocorrelations for the residuals a_i, has approximately χ^2 distribution with K-p-q degrees of freedom. Here, $N = n_1 - 1$ (in our case) equals to the amount of initial data used for the model fitting.

[64] Calculated Q values for every case are shown in column 7 of Table A1. Critical values are obtainable from any table for the χ^2 distribution. The critical value for Q (for K = 24, i.e., 23 degrees of freedom in our case) at the 95% significance level equals to 35.2. Results (Table A1, column 7) show that the test is passed in both cases and the random walk philosophy is acceptable to model global average temperature fluctuations.

[65] The ARIMA(0, 1, 1) model turns out to be a useful tool for representing short-run development of the global average stratospheric and tropospheric temperature anomalies. Note an exceptionally small residual variance for T_{st}, only 4% (column 6 in Table A1). The model can easily be used for short-run predictions of the monthly mean stratospheric temperature anomaly. The dT_{tr} data set has stronger long-range dependence which leads to much worse approximation accuracy (i.e., 35% residual variance).

[66] **Acknowledgments.** The opportunity to use the following online data sets is gratefully acknowledged: MSU data set is obtained from NASA MSFC GHCC www.ghcc.msfc.nasa.gov); Solar irradiance data set (version 19) from PMOD/WRC, Davos, Switzerland, is used containing unpublished data from the VIRGO Experiment on the cooperative ESA/NASA Mission SOHO www.pmodwrc.ch). I thank Ross McKitrick for fruitful discussion and the anonymous reviewers for constructive comments and suggestions. The present work was supported by Estonian Science Foundation grant 4141.

References

Anis, A. A., and E. H. Lloyd, The expected value of the adjusted rescaled Hurst range of independent normal summands, *Biometrika*, *63*, 111–116, 1976.

Bassingtwaighte, J. B., and G. M. Raymond, Evaluating rescaled range analysis for time series, *Ann. Biomed. Eng.*, *22*, 432–444, 1994.

Box, J. E. P., and G. Jenkins, *Time Series Analysis, Forecasting and Control*, (rev. ed.), 575 pp., Holden-Day, Boca Raton, Fla., 1976.

Cahalan, R. F., D. A. Short, and G. R. North, Cloud fluctuation statistics, *Mon. Weather Rev.*, *110*, 26–43, 1982.

Christy, J. R., R. W. Spencer, and W. D. Braswell, MSU tropospheric temperatures: Dataset construction and radiosonde comparisons, *J. Atmos. Oceanic Technol.*, *17*, 1153–1170, 2000.

Coe, M. T., and J. A. Foley, Human and natural impacts on water resources at the Lake Chad basin, *J. Geophys. Res.*, *106*, 3349–3357, 2001.

Cramer, H., and M. R. Leadbetter, *Stationary and Related Stochastic Processes*, John Wiley, New York, 1967.

Davis, A., A. Marshak, W. Wiscombe, and R. Cahalan, Scale invariance of liquid water distribution in marine stratocumulus, I, Spectral properties and stationarity issues, *J. Atmos. Sci.*, *53*, 1538–1558, 1996a.

Davis, A., A. Marshak, W. Wiscombe, and R. Cahalan, Multifractal characterizations of intermittency in non-stationary geophysical signals and fields, in *Current Topics in Non-Stationary Analysis*, edited by G. Trevino et al., pp. 97–158, World Sci., River Edge, N. J., 1996b.

Friis-Christensen, E., and K. Lassen, Length of the solar cycle: An indicator of solar activity closely associated with climate, *Science*, *254*, 698–699, 1991.

Fröhlich, C., and J. Lean, Total solar irradiance variations, in *New Eyes to See Inside the Sun and Stars: Proceedings of IAU Symposium 185*, edited by F. L. Deubner et al., pp. 89–102, Kluwer Acad., Norwell, Mass., 1998a.

Fröhlich, C., and J. Lean, The sun's total irradiance: Cycles, trends and related climate change uncertainties since 1978, *Geophys. Res. Lett.*, *25*, 4377–4380, 1998b.

Ghil, M., Natural climate variability, in *Encyclopedia of Global Environmental Change*, vol. 1, edited by M. MacCracken and J. Perry, John Wiley, New York, 2001.

Hansen, J., R. Ruedy, J. Clascoe, and M. Sato, GISS analysis of surface temperature change, *J. Geophys. Res.*, *104*, 30,997–31,022, 1999.

Hood, L. L., The solar cycle variation of total ozone: Dynamical forcing in the lower stratosphere, *J. Geophys. Res.*, *102*, 1355–1370, 1997.

Hurrell, J. W., K. E. Trenberth, S. J. Brown, and J. R. Christy, Comparison of tropospheric temperatures from radiosondes and satellites: 1979–98, *Bull. Am. Meteorol. Soc.*, *81*, 2165–2178, 2000.

Hurst, H. E., The long-term storage capacity of reservoirs, *Trans. Am. Soc. Civ. Eng.*, *116*, 770–799, 1951.

Huschke, R. E., (Ed.), *Glossary of Meteorology*, 638 pp., Am. Meteorol. Soc., Boston, Mass., 1959.

Intergovernmental Panel on Climate Change, *Climate Change 1995: The Science of Climate Change, Contribution of Working Group I to the Second Assessment Report of the IPCC*, edited by J. T. Houghton et al., 572 pp., Cambridge Univ. Press, New York, 1996.

Jones, P. D., M. New, D. E. Parker, S. Martin, and I. G. Rigor, Surface air temperature and its changes over the past 150 years, *Rev. Geophys.*, *37*, 173–199, 1999.

Kagan, R. L., L. S. Gandin (Ed.), and T. M. Smith (Ed.), *Averaging of Meteorological Fields*, Atmos. Oceanic Ser. Lib., vol. 19, 288 pp., Kluwer, Norwell, Mass., 1997.

Kärner, O., Global temperature deviations as a random walk, *J. Clim.*, *9*, 656–658, 1996.

Kärner, O., and Ü. Rannik, Stochastic models to represent the temporal variability of zonal average cloudiness, *J. Clim.*, *9*, 2718–2726, 1996.

Koscielny-Bunde, E., A. Bunde, S. Havlin, H. E. Roman, Y. Goldreich, and H.-J. Schellnhuber, Indication of a universal persistence law governing atmospheric variability, *Phys. Rev. Lett.*, *81*, 729–732, 1998.

Lovejoy, S., and D. Schertzer, Scale invariance in climatological temperatures and the local spectral plateau, *Ann. Geophys.*, *4B*, 401–410, 1986.

Mandelbrot, B. B., *The Fractal Geometry of Nature*, 460 pp., W.H. Freeman, New York, 1982.

Mandelbrot, B. B., and J. W. van Ness, Fractional Brownian motions, fractional noises and applications, *SIAM Rev.*, *10*, 422–437, 1968.

Mandelbrot, B. B., and J. R. Wallis, Robustness of the rescaled range R/S in the measurement of noncyclic long run statistical dependence, *Water Resour. Res.*, *5*, 967–987, 1969.

McCormick, M. P., L. W. Thomason, and C. R. Trepte, Atmospheric effects of the Mt. Pinatubo eruption, *Nature*, *373*, 399–404, 1995.

Mitchell, J. F. B., The greenhouse effect and climate change, *Rev. Geophys.*, *27*, 115–139, 1989.

Monin, A. S., *Introduction to the Theory of Climate* (in Russian), 246 pp., Gidrometeoizdat, Leningrad, Russia, 1982.

Monin, A. S., and I. L. Vulis, On the spectra of long-period oscillations of geophysical parameters, *Tellus*, *23*, 337–345, 1971.

Pelletier, J. D., The power spectral density of atmospheric temperature from time scales of 10^2 to 10^6 yr, *Earth Planet. Sci. Lett.*, *158*, 157–164, 1998.

Press, W. H., S. A. Teukolsky, V. T. Vetterling, and B. P. Flannery, *Numerical Recipes in FORTRAN*, 2nd ed., Cambridge Univ. Press, New York, 1993.

Robinson, P. M., Log-periodogram regression of time series with long range dependence, *Ann. Stat.*, *23*, 1048–1072, 1995.

Robock, A., Stratospheric control of climate, *Science*, *272*, 972–973, 1996.

Schmitt, F., S. Lovejoy, and D. Schertzer, Multifractal analysis of the Greenland ice-core project climate data, *Geophys. Res. Lett.*, *22*, 1689–1692, 1995.

Spencer, R. W., J. R. Christy, and N. C. Grody, Global atmospheric temperature monitoring with satellite microwave measurements: Method and results 1979–84, *J. Clim.*, *3*, 1111–1128, 1990.

Spencer, R. W., and J. R. Christy, Precision and radiosonde validation of satellite grid-point temperature anomalies, I, MSU channel 2, *J. Clim.*, *5*, 847–857, 1992a.

Spencer, R. W., and J. R. Christy, Precision and radiosonde validation of

satellite grid-point temperature anomalies, II, A tropospheric retrieval and trends during 1979–90, *J. Clim.*, *5*, 858–866, 1992b.

Staehelin, J., N. R. P. Harris, C. Appenzeller, and J. Eberhard, Ozone trends: A review, *Rev. Geophys.*, *39*, 231–290, 2001.

Taqqu, M. S., and V. Teverovsky, Semi-parametric graphical estimation techniques for long-memory data, *Lect. Notes Stat.*, *115*, 420–432, 1996.

Taqqu, M. S., V. Teverovsky, and W. Willinger, Estimators for long-range dependence: An empirical study, *Fractals*, *3*, 785–798, 1995.

O. Kärner, Tartu Observatory, Tõravere 61602, Estonia. (olavi@aai.ee)